17th World Conference on Earthquake Engineering, 17WCEE
Sendai, Japan - September 13th to 18th 2020

SPATIAL AND TEMPORAL VARIATION IN THE CORRELATION OF SEISMIC RESPONSE WITH THE SPECTRAL ACCELERATION

A. Athanatopoulou[(1)], A. Papasotiriou[(2)], K. Kostinakis[(3)]

[(1)] *Professor, Aristotle University of Thessaloniki, minak@civil.auth.gr*
[(2)] *Ph.D. candidate, Aristotle University of Thessaloniki, apapasso@civil.auth.gr*
[(3)] *Assistant Prof., Aristotle University of Thessaloniki, kkostina@civil.auth.gr*

Abstract

Spectral acceleration at the fundamental period of the structure $S_a(T_1)$ is the most widely used structure-specific seismic Intensity Measure (IM) for the assessment of the structures' seismic damage. The vast majority of the modern seismic codes define earthquake hazard in terms of spectral acceleration, and $S_a(T_1)$ is often used as a default seismic intensity scaling parameter for time history analyses. The high correlation between $S_a(T_1)$) and common seismic Response Measures (RMs) in low-rise structures has been extensively documented in present-day research.

To further investigate the relation between spectral acceleration and the seismic response of the structure, the correlation between $S_a(T)$ and a set of common RMs was examined, not only at specific periods (such as T_1, T_2 etc.) but at the whole period range from 0 sec to 20 sec. This allows determining the characteristics of the "resonance" at the natural frequencies, such as the bandwidth of the main high-correlation lobe around T_1, as well as the presence of secondary regions of high correlation. The response of a wide range of planar frames was simulated using the non-linear dynamic analysis (implemented with Opensees software), with a suite of 60 appropriately selected ground motion records. In total, 32 basic R/C frame configurations (moment frames and dual systems) were studied, both as bare and infilled frames, each one with 12 different infill types (in total 416 different models), for 10 different seismic intensity levels. For each model, a variety of local and global RMs were calculated, both at the storey level and globally. The chosen RMs are based on displacement demands (such as maximum and average interstorey drift), on local deformation demands (rotation/curvature ductility demands) and on the dissipated energy per element due to nonlinear response. The correlation between the above RMs and $S_a(T)$ was calculated for a large number of periods, ranging from 0 sec to 20 sec, with a step of 0.01 sec.

In most cases, the results reveal a peak of particularly high correlation at the region of T_1, while in some cases secondary peaks appear at higher natural periods. However, each model and each RM exhibit individual characteristics with regard to the peak correlation factor, the sharpness of the correlation at T_1 and the overall bandwidth of high correlation. More interestingly, the frequency content of high correlation is found to change between successive storeys, with RMs at higher storeys exhibiting high correlation with $S_a(T_1)$ at much lower periods. This phenomenon was observed for all the frames, and in many cases, it is strong enough to cause a shift in the peak correlation period from T_1 (at lower storeys) to T_2 (at higher storeys). This spatial variation in the correlation was found to be a general characteristic in the post-elastic response domain and its magnitude is strongly associated with the characteristics of both the main bearing structure and the infill. Additionally, the elongation of the apparent fundamental period due to the post-elastic response (temporal variation) was found to have a distinctive effect on the bandwidth of high correlation, which was more pronounced in the case of infilled frames.

Keywords: masonry infills; performance based earthquake engineering; seismic damage; reinforced concrete buildings

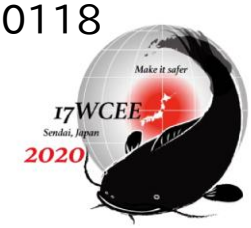

1. Introduction

Spectral acceleration at the fundamental period of the structure $S_a(T_1)$ is a widely used structure-specific seismic intensity measure (IM) for the assessment of the structures' seismic damage. $S_a(T_1)$ has been repeatedly found to be the seismic parameter that has the highest correlation with the structural damage (e.g. [1, 2, 3, 4]), and is being regarded as an "efficient" and "sufficient" [5] parameter in predicting the seismic performance of a building. However, many researchers have highlighted the deficiencies of $S_a(T_1)$ as an IM, often with regard to mid-rise structures (e.g.[5, 6, 7]) and proposed more complex spectrum-based IMs, either of the scalar type [6, 7, 8] or of the vector type [9, 10], in an attempt to produce even more robust IMs. To this aim, the main strategy is to take into account the spectral acceleration not only at the fundamental period of the structure but also at higher natural periods, as well as to account for other parameters such as the distance from the source, the damping ratio of the structure etc. Apparently, the respective research is based on the seemingly self-evident premise that the seismic response of the structure is mainly determined by resonance phenomena, taking place at the natural frequencies of the structure. Nevertheless, this assumption can be questioned, not only because the natural frequencies of the structure vary significantly during the post-elastic response, but also by the very shape of the elastic response spectrum, which flattens substantially at higher damping ratios.

As the quest for more efficient spectrum-based intensity measures continues, it becomes apparent that there are aspects of the relationship between spectral acceleration and the seismic response that are still poorly understood. This is true especially with regard to characteristics such as the maximum correlation factor and the period on which it occurs, the bandwidth of the main high-correlation lobe and the assumed resonance phenomena, the contribution of the higher modes to the structural damage, the effect of the shifting of the natural frequencies in the post elastic response etc. With the objective of investigating these topics, the authors have developed a method for calculating the correlation between S_a and the structural response as a pseudo-continuous variable, across a wide spectrum range. The relevant research revealed interesting details on all the aforementioned aspects of the relationship between spectral acceleration and the structural response, which have broader relevance to the earthquake-resistant design of the structures. However, the present study focuses on two specific phenomena that affect the relation between S_a and the seismic response of the structure, namely the shift of the high-correlation period range to higher frequencies at higher storeys of the building (spatial variation) and the expansion of the high-correlation period range due to the shifting of the fundamental frequency as the damage progresses (temporal variation).

This investigation is based on the results of a large number of non-linear dynamic analyses of planar frames. In total, 32 basic R/C frame configurations were studied (eight different frame types, comprising moment frames and dual systems, with frames of 2, 4, 6 and 8 storeys each). Moreover, 12 different infill types of uniform distribution (four categories of different strength and three categories of different ductility of infill walls) were also considered. For the modeling of the buildings' nonlinear behavior, beam-column elements with distributed plasticity and fiber sections were used, while the equivalent diagonal strut model was adopted for the modeling of the infill. The seismic response was simulated with the Opensees software, by employing the nonlinear time-history analyses for a suite of 60 appropriately selected real ground motions records scaled to 10 different seismic intensity levels, resulting in a total of 249,600 (4 height groups X 8 frame types X (bare frames + 12 infill types) X 60 records X 10 seismic intensities) time-history analyses.

2. Investigated R/C frames and N/L dynamic analyses modeling parameters

Four groups of frames with a height of two, four, six and eight floors were investigated. Each group consists of five moment frames with columns of different section size and three dual systems with shear walls of different width, as follows:

Frame type 1: Moment frames designed for a low seismic load, according to the old Greek seismic code.

Frame type 2: Moment frames designed according to EC-8 [11], but without the capacity design of the columns.

Frame type 3: Moment frames fully complying to EC-8, with the smallest possible column sections.

Frame type 4: Moment frames with overdesigned columns, fully conforming to EC-8. The columns in this category have a section width 50% larger than that of the corresponding columns of frame type 3.

Frame type 5: Moment frames with overdesigned columns, fully complying to EC-8. The column sections in this category have double the width of the corresponding column sections in category 3.

Frame type 6: Dual systems, designed according to EC-8, with one slender shear wall. The wall section was chosen so that the sum of the moments of inertia of the vertical elements on the first floor equals the corresponding sum of the frames of type 4.

Frame type 7: Dual systems, designed according to EC-8, with a strong shear wall. The wall section was chosen so that the sum of the section modulus of the vertical elements of the first floor equals the corresponding sum of the frames of type 4.

Frame type 8: Dual systems, designed according to EC-8, with a shear wall even stronger than that of frame type 7.

For the presentation of the research results the following notation for the investigated structures will be used: each frame will be denoted by two numbers (i-j), where the first number (i) denotes the number of the storeys and the second number (j) denotes the abovementioned frame type.

The seismic load for designing the frames complying with EC-8 [11] was calculated in accordance with the Greek annex, for soil type “C” and seismic zone II. In all cases, the reinforcing details and, therefore, the hysteretic behavior of beams and columns fulfill the requirements of EC-2 [12] and EC8 [11]. Furthermore, special care was taken not to overdesign the frames. The design procedure of the frames was based on the linear method of analysis (modal analysis), in accordance with EC-8 and the Greek national annex.

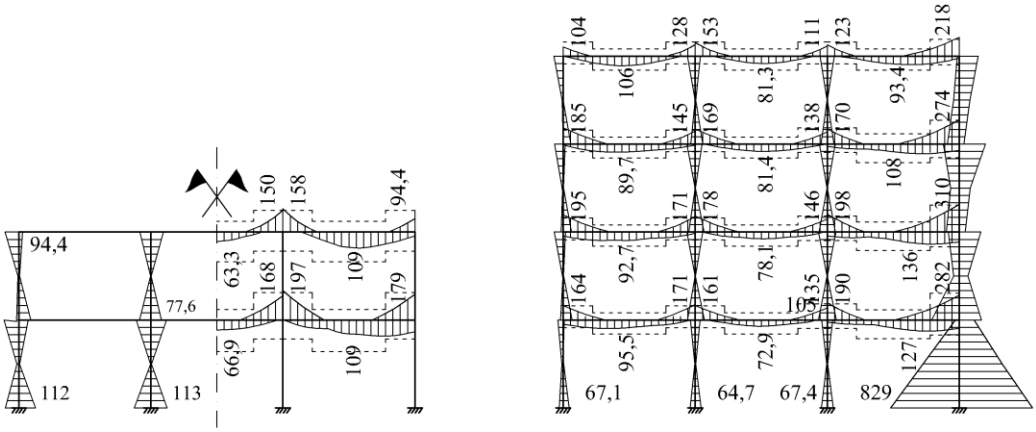

(a) (b)

Fig. 1 – Frame outline and envelopes of the design moments for frames 2-2 (a) and 4-6 (b)

To simulate the seismic response of the frames, non-linear time history analyses were performed for both the bare and the infilled frames using Opensees. With regard to the infilled frames, four different levels of masonry panel strength and three levels of infill ductility were considered (Table 1) in order to cover the most common types of UnReinforced Masonry (URM) infill, including infill walls with openings. The mechanical characteristics of the infill panels were specified in terms of interstorey drift and masonry shear

force and they attain the predetermined values shown in Table 1 in all the frame types, regardless of the frame layout. Additionally, the frame members were carefully modeled in order to preclude secondary characteristics -not included in the investigation- from influencing the analysis results.

Table 1 – Overview of the defining parameters of the idealized backbone curve for the 12 infill types

Table notations: P_0-strut compression strength, P_u-residual strut strength, ε_0-strut strain at P_0, ε_u-strut strain at P_u, V_0-panel shear strength (corresponding to P_0), V_u-panel residual strength (corresponding to P_u), δ_0 story drift ratio corresponding to ε_0, δ_u story drift ratio corresponding to ε_u,.

No	Strength category	Plasticity category	equivalent strut properties				infill panel properties			
			P_0 (kN)	P_u (kN)	ε_0 (‰)	ε_u (‰)	V_0 (kN)	V_u (kN)	δ_0 (‰)	δ_u (‰)
1	1	1	40	0	1.85	5.54	33.3	0	4.0	12
2	1	2	40	0	2.77	12.46	33.3	0	6.0	27
3	1	3	40	0	3.69	22.15	33.3	0	8.0	48
4	2	1	102	0	1.85	5.54	84.8	0	4.0	12
5	2	2	102	0	2.77	12.46	84.8	0	6.0	27
6	2	3	102	0	3.69	22.15	84.8	0	8.0	48
7	3	1	176	0	1.85	5.54	147	0	4.0	12
8	3	2	176	0	2.77	12.46	147	0	6.0	27
9	3	3	176	0	3.69	22.15	147	0	8.0	48
10	4	1	260	0	1.85	5.54	216	0	4.0	12
11	4	2	260	0	2.77	12.46	216	0	6.0	27
12	4	3	260	0	3.69	22.15	216	0	8.0	48

The non-linear time history analyses were performed using a sample of 60 normalized ground motion records obtained from the PEER strong motion database [13]. The records have been appropriately selected to conform to the elastic spectrum for soil type C according to EC8 (so as to correspond to the design spectrum used in frame design, Fig.2). To this end, the geometric mean square error (MSE) between the spectral acceleration of each record and the target spectrum in the range 0.15sec ~ 5.0sec was used as the main selection criterion, while various seismic parameters were utilized to additionally confine the selected set. More specifically the following limiting values were adopted: magnitude M5.5 ~ M8.5, epicentric distance R_{jb} = 10 km ~ 50 km, mean shear wave velocity at the upper 30 m $V_{s,30}$ = 240 m/sec ~ 400 m/sec and significant duration $d_{5\text{-}95}$ = 10 sec ~ 30 sec. The aforementioned values were chosen in order to exclude unlikely events, and also as a means for better matching to the target spectrum. The final suite comprises of both far-fault and near-fault events and covers uniformly a rather wide range of earthquake characteristics regarding the frequency content and the most common intensity measures. The average spectrum of the suite matches well the target spectrum, and the variance of the spectral acceleration is symmetric and even across all periods (Fig.2(b)).

The records have been scaled to 10 different intensity levels, ranging from very weak excitations (5% of the design earthquake in level 1), up to extremely strong excitations (225% of the design earthquake in level 10). The criterion adopted for scaling the records was the minimization of the geometric MSE from the

target spectrum (MSE scaling [14]). The MSE was calculated with a constant weight factor in the period range 0.3s-4.0s, which exceeds by far the range of the natural periods of the models under consideration. The resulted scaled suites have an almost normal distribution of $S_a(T)$ values across all periods, and for intensity level 5 the average spectrum matches almost perfectly the target spectrum. The main objective of the records scaling is to preclude the variance in the intensity of the excitations from affecting the correlation between $S_a(T)$ and the seismic response. As a result, the acquired correlation factors are determined mainly by the variance in the frequency contents of the records, and not by the variance in the seismic intensity itself. The scaling of the records also allows to examine the change in the correlation between $S_a(T)$ and the seismic response as the seismic intensity increases, as well as to attribute certain characteristics of the seismic response to specific seismic intensity levels. A side-effect of the scaling, however, is that the correlation factors found in the present study are lower than those reported in most of the relevant literature (e.g. [1-5]).

The frames were modeled using nonlinear force based beam-column elements with distributed plasticity [15] and fiber sections, to accurately simulate the post-elastic behavior of the structural elements, as well as the interaction between axial force and biaxial moment. In modeling the floor diaphragmatic action care was taken not to affect the behavior of the beams by constraining their axial deformation (because of the axial-moment interaction). Uniaxial materials "comcrete01" and "steel4" were adopted for modeling the hysteretic behavior of the concrete and the reinforcing steel respectively. The infill walls were modeled using the equivalent strut method. Each infill panel is modeled as a pair of diagonal compression-only struts, the mechanical characteristics of which were calculated using the formulae proposed by Stafford & Carter [16] and Mainstone [17] and correspond to the values listed in Table 1. Finally, the "pinching4" hysteretic law was used to define the nonlinear behavior of the struts, as it has been shown to be the most accurate model available in Opensees for implementing the equivalent strut method [18-20].

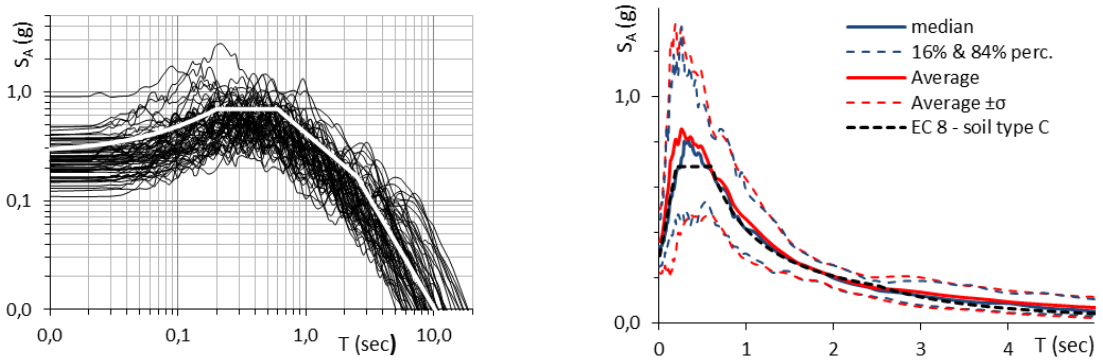

(a) (b)

Fig. 2 – (a) Response spectra (5%) of the un-scalled earthquake records (EC-8 elastic spectrum is superimposed as a white line), (b) 16, 50 and 84 percentile spectra of the scaled records.

3 Assessment of the seismic response of the structures

The seismic response of the frames was evaluated using local and global response measures, namely, (i) the average interstorey drift ratio (AIDR), (ii) the maximum interstorey drift and (iii) the deformation demand on the columns. The average interstorey drift ratio was calculated as the ratio of the maximum top displacement to the total height of the structure. It is the simplest of the response measures, suitable only for a coarse estimation of the seismic response of the frames. However, in the context of the present study AIDR is of high importance, as it has been found to exhibit the highest correlation factors with $S_a(T)$ among any other of the response measures under investigation, always at the apparent fundamental period of the structure. Consequently, the correlation between AIDR and $S_a(T)$ can be used to determine the apparent fundamental period of the structure.

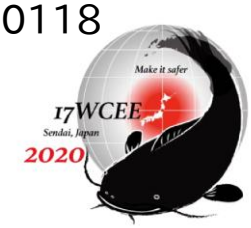

The interstorey drift ratio (Δ), calculated at every storey as the ratio of the maximum interstorey drift to the storey height, is a commonly used coarse damage measure, which represents the deformation demand at the storey level. The maximum interstorey drift ratio (Δ_{max}) represents the maximum storey-level deformation demand on the building, and it is generally considered an effective indicator of the global structural and nonstructural damage of R/C buildings (e.g. [21-23]). Interstorey drift (Δ) is the main response measure used in the present study to investigate the spatial and temporal variance of the response - $S_a(T)$ correlation.

With regard to the column deformation demand, the peak absolute curvature of the columns is used to derive a storey-level damage measure for assessing the seismic response of the structure. This measure is calculated as the weighted average curvature of the storey columns, according to Eq. (1).

$$\Phi = \sum_{i=1}^{N} \left(\frac{\Phi_{i,u} + \Phi_{i,o}}{2 \cdot \Phi_{i,y}} \cdot \frac{w_i}{\sum_{i=1}^{N} w_i} \right) \quad (1)$$

$\Phi_{i,o}$ and $\Phi_{i,u}$ are the peak curvature at the top and the bottom of column i respectively, $\Phi_{i,y}$ is the curvature at yielding point, and w_i is the section modulus of the respective column. Φ has the form of a non-cumulative damage measure, however, it represents the average residual strength of the storey columns. In moment frames conforming to capacity design criteria, Φ should take a value larger than 1 only at the ground floor. The ratio of the column section modulus to the sum of all the column moduli is a weight factor approximating the degree to which each column contributes to the storey shear strength. So, for storeys above ground level, in which the curvature at the top and the base of the columns are roughly the same, a Φ value less than 1 represents the storey shear force demand to capacity ratio. Also, Φ values larger than 1 may signify the formation of a storey mechanism. As in the case of interstorey drift, the maximum Φ value that appears on a building (Φ_{max}) is used as a global response measure.

4. Methodology and general observations

The correlation coefficient (r(T)) between the aforementioned response measures and the spectral acceleration was calculated for each one of the 416 models (4 height groups X 8 frame types X (bare frames + 12 infill types)) as a function of the spectral period in the range of 0-20sec (Fig.3). In fact, r(T) is a set of pseudo-continuous data, acquired by repeatedly calculating the correlation between the response measures and the spectral acceleration for a large number of consecutive periods separated by a very small interval. Sensitivity analysis was conducted in order to certify that the period interval is small enough not to affect the actual correlation values, as well as to determine proper values for the damping ratio used in the calculation of the response spectrum. The correlation coefficient (r(T)) was calculated independently for the 10 different seismic intensity levels, thus resulting in 4160 different correlation functions for each response measure. Pearson correlation was preferred, as the analysis of the results has revealed the existence of a particularly strong linear component of association between the $S_a(T)$ and response quantities. Spearman (rank) correlation results were found to be remarkably similar to the Pearson results (average difference in maximum correlation values +3.4%), and so of no particular interest.

In most cases, the correlation between spectral acceleration and the seismic response shows a distinct peak of a relatively high r(T) value, usually in the region of the fundamental period of the structure. The actual peak correlation value, as well as the width of the main high-correlation lobe, were found to depend greatly on the characteristics of the frames, the infill type and the intensity level of the excitation, and to vary significantly among different models and different response quantities. In some cases, smaller peaks can be detected at periods related to other modes, however, the corresponding correlation coefficient is usually too small to explicitly attribute these peaks to the participation of the corresponding modes (Fig.3). Regions of negative correlation are commonly observed outside the main high-correlation lobe (Fig.3), as a result of the interdependency between the spectral acceleration values $S_a(T)$ within each spectrum. Because of this interdependency there is a substantial possibility for spurious correlation to arise. Consequently, the

correlation between a response quantity and the spectral acceleration should be taken as evidence of a causal relation only in the case of a high-correlation lobes corresponding to natural periods of the structure.

Lobes of high correlation, coinciding with some natural period of the structure are typical for all of the frames and the RMs under investigation. However, AIDR is the RM most highly correlated with $S_a(T)$, and its peak correlation always takes place at the apparent fundamental period of the structure. As a result, the period of peak AIDR correlation, denoted herein as T_c, is regarded as a reliable indicator of the average apparent fundamental period for the set of time-histories under consideration. For very weak excitations (seismic intensity level 1) T_c was found to coincide with T_1 as calculated by the modal analysis. As the seismic intensity increases, so does T_c, and the relation between the two is in most cases almost linear. Contrary to AIDR, Δ_{max} and Φ_{max} of higher frames (frames 6-1, 8-1, 8-2, 8-3 of the present study) can exhibit a correlation peak at a higher natural period (e.g. Fig.4, frame 8-1). This usually comes with a much wider high-correlation bandwidth, which extends to the period T=0.

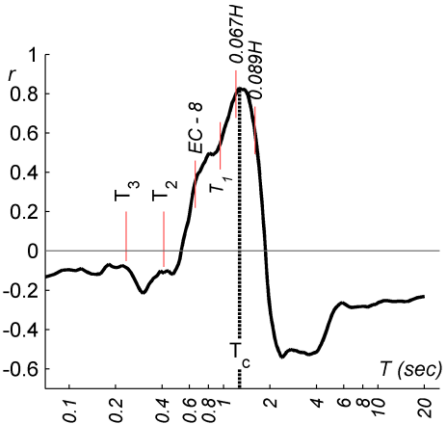

Fig. 3 – Correlation curve r(T) between spectral acceleration and AIDR of bare frame 6.3 (six-storey moment frame), for intensity level 5 (corresponding to the design seismic action). T_1~T_3 are the first three natural frequencies, as calculated by modal analysis. 0.067H, 0.089H and EC-8 are predictions of T_1 based on [24], [25] and [11] respectively.

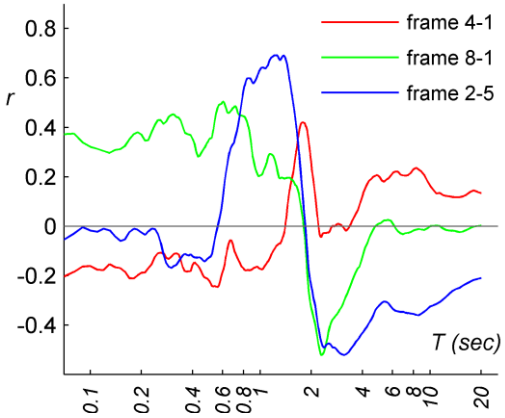

Fig. 4 – Examples of non-typical correlation graphs (intensity level 100%):
- bare frame 4-1, Δ_{max}: poor correlation, spurious correlation for periods over 4sec
- bare frame 8-1, Φ_{max}: higher modes dominate in the correlation
- bare frame 2-5, Δ_{max}: single mode, wide bandwidth correlation

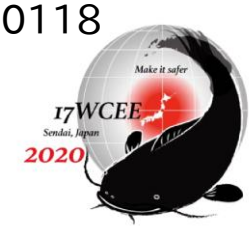

5. Temporal variation

The primary causes of the increase in the bandwidth of the high correlation between RMs and $S_a(T)$ (e.g. Fig.4, frame 2-5) are the variance in the characteristics of the response spectra of the 60 seismic motions, as well as the change of the building's natural period due to inelastic deformations within each time history. The second one, hereinafter called "temporal variation", leaves a distinctive trace on the r(T) diagram, in the form of one or more secondary lobes, attached to the side of the main high-correlation lobe (Fig.5). In the bare frames, this secondary lobe tends to roughly coincide with the elastic fundamental period of the structure (Fig.5 (a) and (b)). In the case of the infilled frames, the secondary lobe can appear at either side of the main lobe, or at both sides simultaneously (Fig.5 (c) and (d)). In this case, the higher secondary lobe roughly coincides with the maximum apparent fundamental period of the respective bare frame (which corresponds to the máximum lateral deformation of the structure). In Fig.5(c) & (d) the r(T) curves of the respective bare frames are also depicted to allow for a direct comparison with the right secondary lobe in the r(T) curve of the infilled frames. A thorough examination of the results confirmed that these secondary lobes are not a side effect of the interdependence between $S_a(T)$ at different periods, but rather an actual effect of the spectral acceleration at the specific periods on the DMs. Quite naturally, not all frames exhibit distinctive secondary lobes as in the examples of Fig.5. In many cases, the side lobes are either completely absent (as in Fig.4, frame 4-1), or completely blended with the main high-correlation lobe. Moreover, as already mentioned, other phenomena -the spatial variation included- can also cause an expansion of the main high-correlation lobe, rendering in some cases difficult -if not impossible- to identify the effect of the temporal variation.

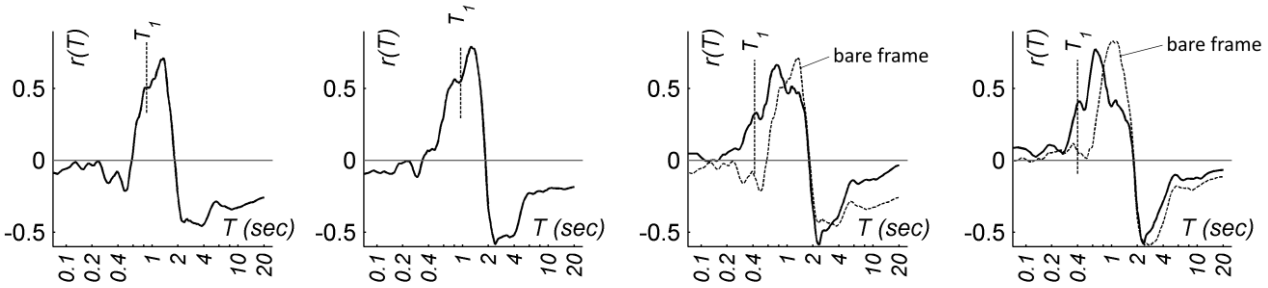

(a) (b) (c) (d)

Fig. 5 – Characteristic examples of secondary lobes in the correlation between Δ_{max} and $S_a(T)$. (a) and (b) bare frames 2-2 and 3-3, (c) frame 2-2 with infill type 8, (d) frame 3-4 with infill type 3

The existence of the secondary high-correlation lobes seems at first counterintuitive. Since the DMs attain their value at a specific point in each time-history, they were expected to correlate with the $S_a(T)$ at the apparent period of the structure at this very point. And, as most DMs are associated -more or less- with the maximum lateral deformation of the structure, the maximum correlation should take place at the maximum apparent natural period. Moreover, since all the records are scaled, DMs attain their value well within the post-elastic response domain for all the 60 time-histories of each set of dynamic analyses. The existence, however, of the secondary lobes suggests that events taking place at the early stages of the excitation -well before the apparent natural period attains its peak value- can affect the maximum response of the structure. In many of the bare frames (e.g. Fig.5 (a) and (b)), the spectral acceleration at the elastic fundamental period ($S_a(T_1)$) appears to contribute significantly to the DMs, indicating that narrow-band resonance is the main mechanism that transfers seismic energy into the structure. Apparently, the same is true for most of the infilled frames, which, however, exhibit a much lower T_1 than the respective bare frames, due to their higher initial stiffness. In many of the infilled frames, the maximum correlation between $S_a(T)$ and the DMs occurs at a period lower than the period corresponding to the maximum lateral deformation of the structure. This period corresponds approximately to the failure of the infill panels, implying that in frames with strong infill walls the most important event that determines the DMs is the infill failure and not the events that follow it leading to the final increase in the deformation of the structure. As is to be expected, the transition in the r(T)

curve shape of the frames happens gradually as the infill strength increases, and, for low infill strength, many of the aforementioned characteristics are not recognizable (Fig.6).

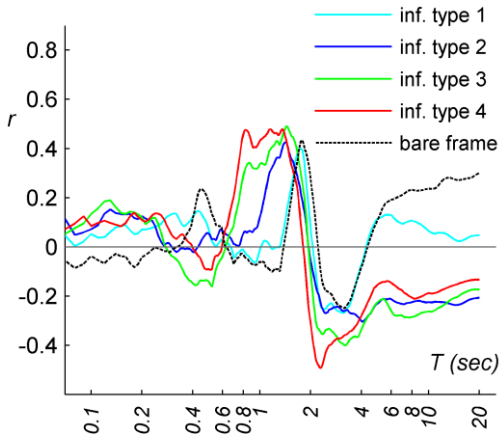

Fig. 6 – Example of the gradual change in the r(T) curve as the infill strength increases. Frame 8-8, Φ_{max}. The bare frame exhibits a minor peak corresponding to the second mode, which disappears in the infilled frames.

6. Spatial variation

Storey-level response quantities (interstorey drift, average deformation of the storey columns) are the basis for extracting global response measures of the building, such as Δ_{max} and Φ_{max}. The correlation between these storey-level quantities and the spectral acceleration was found to vary between different floors of the same structure. More specifically, as we move to higher floors, the correlation with $S_a(T)$ gets progressively stronger in the period range below T_c. For many structures, this change is quite pronounced and can eventually lead to a shift of the maximum correlation peak from T_c to a lower period, and sometimes to the period of a higher mode (Fig.7). In some cases, the maximum correlation factor (r_{max}) tends to increase at the higher storeys and occasionally exceeds the respective r_{max} value for the ground floor. This phenomenon -hereinafter called "spatial variation"- appears in all the frames and the response quantities under investigation regardless of the characteristics of the main bearing structure and the presence of infills or not. The spatial variation is determined to a significant degree by the structural layout of the frames. Dual systems tend to experience much smaller variation, while in moment frames the presence of extremely strong columns can also reduce the variation. Frames with a different number of storeys exhibit a different amount of spatial variation too. Finally, the reduction in the column section size at the upper floors tends to cause a slight reduction in the correlation with the higher frequency content, however, the overall effect is not significant. In bare frames, the transition in the correlation with the high-frequency content of the spectrum takes place gradually (Fig.7(a)), while in the infilled frames the change happens rather abruptly, at the storeys where the damage is concentrated (Fig.7(b)).

The spatial variation in the correlation between the RMs and $S_a(T)$ cannot be explained on the basis of the elastic modal analysis since the participation factors of higher modes are particularly small. The variation remains limited as long as the structure response stays within the elastic response domain and thereafter increases rapidly with the seismic intensity. So, the spatial variation is a phenomenon that appears exclusively in the post-elastic response. It affects mainly the moment frames (Fig.8), and it implies that excitations with different frequency content can cause damage to different parts of a structure. While this is certainly not a new finding, the present study demonstrates that the spatial variation has certain, quantifiable characteristics, which are determined by the properties of the structure. The spatial variation can affect the global DMs that are derived from storey-level DMs, since they get their maximum value -in the general case- on different storeys for different ground motion records. This is illustrated in Fig.7, by the dashed Δ_{max} curve which does not coincide with any of the four Δ curves. As a result, global DMs tend to exhibit a broader

bandwidth of high correlation than the local DMs at the ground storey. In higher frames, the high correlation area of the global RMs can expand all the way until the period T=0 (e.g. Fig.4, frame 8-1). In fact, spatial variation was found to be the cause for the very wide high-correlation lobes and the domination of higher modes in the case of frames 6-1, 8-1, 8-2 and 8-3. In these frames, the local DMs of the lower storeys continue to exhibit narrow correlation lobes with a peak at T_c, however, the global DMs often come from the higher storeys, and thus they are affected by $S_a(T)$ in a wide period range. To a lesser extent, this effect appears in all the other eight-storey frames (frames 8-4 to 8-8) causing the global RMs to have a lower r_{max} value than the local RMs. These findings suggest that the spatial variation may lay behind the poor correlation between DMs and $S_a(T_1)$ in mid-rise buildings.

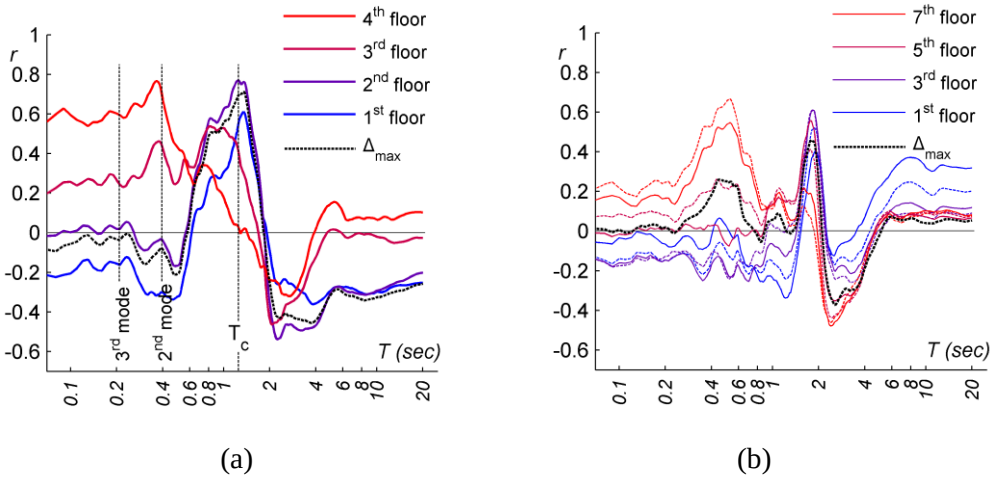

(a) (b)

Fig. 7 – Correlation r(T) between spectral acceleration and interstorey drift (Δ) for frame 4-2. The periods of 2nd and 3rd mode are approximately estimated by referring T_1 to T_c. (a): bare frame, (b): infill type 6.

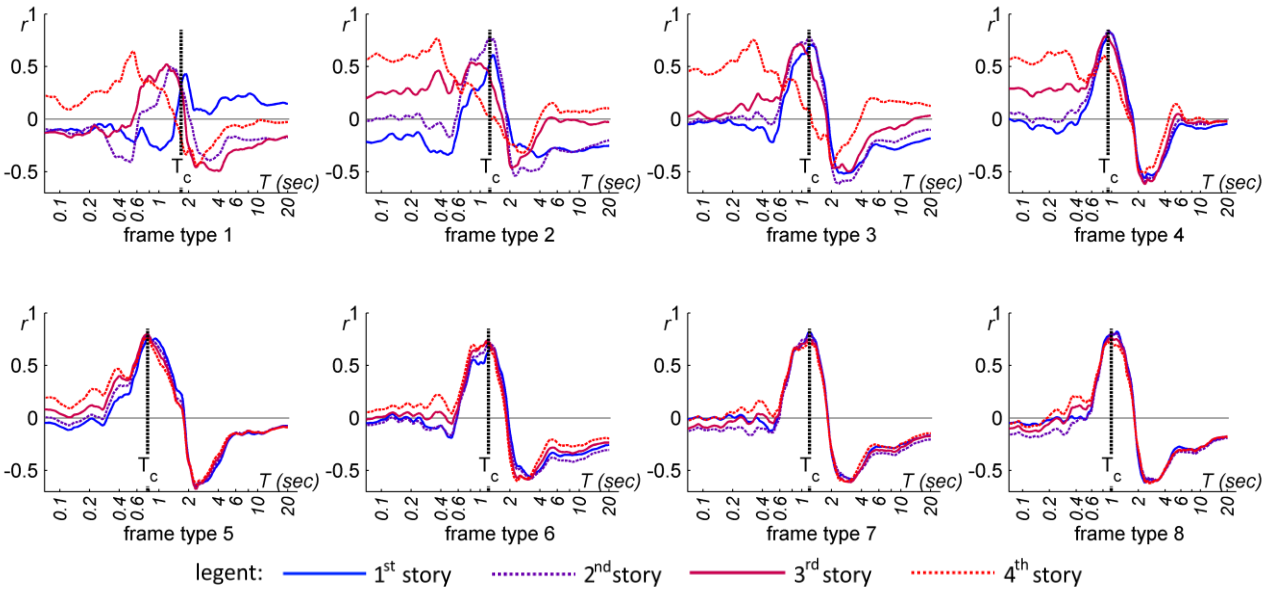

Fig. 8 – Correlation r(T) between spectral acceleration and interstorey drift on every storey of the four-storey bare frames.

7. Conclusions

The present paper investigates the correlation between the spectral acceleration and the seismic response of planar multistorey R/C buildings with various masonry infill panels of uniform distribution. Both storey-level and global RMs are calculated for each frame for 10 different seismic intensity levels. The correlation between these parameters was computed as a pseudo-continuous data set in the period range 0sec ~ 20 sec, allowing a comprehensive investigation of the spectral content that affects the seismic response. Based on the results of the present investigation, the following conclusions can be drawn:

- The period of peak correlation between $S_a(T)$ and AIDR was found to be a reliable estimation of the average fundamental period of the structure for low-rise to mid-rise frames.
- In most cases, RMs were found to correlate with $S_a(T)$ in a narrow-band area, suggesting that resonance is the main mechanism that drives the transfer of seismic energy to the structure. However, the apparent fundamental period of the structure shifts significantly during each excitation, and it is impossible to accurately predict the actual period of peak correlation by using empirical formulae.
- The main high-correlation lobe usually covers the whole period range of the shifting fundamental period, and in many cases shows secondary peaks, which suggest that events that take place at the early stages of the excitation can affect the maximum response of the structure. Especially in the case of frames infilled with strong panels, the peak correlation tends to appear at a lower period corresponding to the failure of the infill, and not at the period corresponding to the maximum structural damage.
- The correlation between storey-level quantities and the spectral acceleration was found to be different on different storeys of the same structure. More specifically, as we move to higher floors, the correlation for periods smaller than T_c gets progressively stronger. This spatial variation in the correlation between $S_a(T)$ and RMs is more pronounced in moment frames than in dual systems. In higher frames, this phenomenon affects strongly the correlation between global DMs and $S_a(T)$, causing -among others- a drop in the peak correlation value.
- According to the findings of the present study, it is possible to derive more efficient spectrum-based IMs, either of scalar or vector type, by sampling $S_a(T)$ in multiple, well-defined periods, in order to account for the two aforementioned phenomena. However, accurate prediction of the apparent fundamental period of the structure is of paramount importance, since the correlation peak is -in most cases- particularly narrow.

8. Acknowledgments

Results presented in this work have been produced using the AUTH Compute Infrastructure and Resources. The earthquake records were obtained from the Pacific Earthquake Engineering Research Center (PEER) database. Time-history analyses were performed using OPENSEES software developed at Berkley University.

9. References

[1] Elenas A (1997): Interdependency between seismic acceleration parameters and the behaviour of structures. *Soil Dyn Earthq Eng,* **16**, 317-322.

[2] Elenas A, Meskouris K (2001): Correlation study between seismic acceleration parameters and damage indices of structure. *Eng Struct,* **23**, 698-704.

[3] Kostinakis K, Athanatopoulou A, Morfidis K (2015): Correlation between ground motion intensity measures and seismic damage of 3D R/C buildings. *Engineering Structures*, **82**, 151-167.

[4] Kostinakis K, Athanatopoulou A (2015): Evaluation of scalar structure-specific ground motion intensity measures for seismic response prediction of earthquake-resistant 3D buildings. *Earthquake and Structures*, **9**(5), 1091-1114.

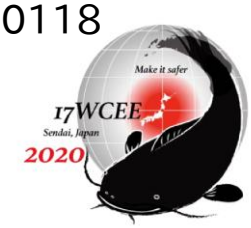

[5] Luco N, Cornell CA (2007): Structure-specific scalar intensity measures for near-source and ordinary earthquake ground motions. *Earthquake Spectra*, **23**(2), 357–392.

[6] Luco N, Manuel L, Baldava S, Bazzurro P (2005): Correlation of damage of steel moment-resisting frames to a vector-valued set of ground motion parameters. *9th International Conference on Structural Safety and Reliability (ICOSSAR05),* Rome, Italy

[7] Yahyaabadi A, Tehranizadeh M (2011): New scalar intensity measure for near-fault ground motions based on the optimal combination of spectral responses. *Scientia Iranica*, **18**(6) 1149-1158.

[8] Mehanny S (2009): A broad-range power-law form scalar-based seismic intensity measure. *Engineering Structures*, **31**(7), 1354-1368.

[9] Bojórquez E, Iervolino I (2001): Spectral shape proxies and nonlinear structural response. *Soil Dynamics and Earthquake Engineering*, **31**(7), 996-1008.

[10] Kohrangi M, Bazzurro P, Vamvatsikos D (2016): Vector and scalar IMs in structural response estimation, Part I: hazard analysis. *Earthquake Spectra*, **32**(3), 1507-1524.

[11] Eurocode 8 (EN 1998-1), Design provisions for earthquake resistance of structures, European Committee for Standardization, 2005.

[12] Eurocode 2 (EN 1992-1-1), Design of concrete structures - General rules and rules for buildings, European Committee for Standardization, 2005.

[13] Pacific Earthquake Engineering Research Centre (PEER). *Strong Motion Database*. http://peer.berkeley.edu/smcat/. 2003.

[14] Michaud D, Léger P (2014): Ground motions selection and scaling for nonlinear dynamic analysis of structures located in Eastern North America. *Canadian Journal of civil engineering*, **41**(3), 232-244.

[15] Scott M H (2011). Numerical integration options for the force-based beam-column element in OpenSees. *Opensees Wiki*, http://opensees.berkeley.edu.

[16] Stafford S B, Carter C (1969): A method of analysis for infilled frames. *Proceedings of the institution of civil engineers*. **44**(1), 31-48

[17] Mainstone R J (1971): On the stiffness and strengths of infilled frames. *Proceedings of the Institution of Civil Engineers.* IV-7360S, 57-9.

[18] Pragalath H, Karthick H., Pratap S., Sriraman M., Madhura S. (2015). Selection of Infill Wall Material Modelling for Seismic Excitation. *International Journal of Applied Engineering Research*, **10**(17), 37225-37234

[19] Durai T. N. P., Arunachalam J., Karthich L. A., Pragalath D. H., Iswarya D., Singh, R. (2016). Computational Model for Infill Walls under Cyclic Loads. *International Journal of Applied Engineering Research*, **11**(4), 2786-2790.

[20] Mohammad N., Liberatore L., Mollaioli F., Tesfamariam S. (2017): Modeling of Masonry Infilled RC Frames Subjected to Cyclic Loads: State of the Art Review and Modelling with OpenSees. *Engineering Structures* 150. Elsevier Ltd:599–621.

[21] Gunturi SKV, Shah HC (1992): Building specific damage estimation. *Proc. of 10th World Conference on Earthquake Engineering*, Madrid, Spain. Rotterdam: Balkema: 6001–6.

[22] Naeim F (2001): *The seismic design handbook*, 1st Ed., Kluwer Academic, Boston, MA.

[23] Priestley MJ N, Calvi GM, Kowalsky MJ (2007): Displacement-based seismic design of structures, *IUSS Press*, Pavia, Italy

[24] Chopra A K, Goel R K. (2000): Building Period Formulas for Estimating Seismic Displacements, *Earthquake Spectra*, **16**(2): 533–536.

[25] Crowley H, Pinho R. (2006): Simplified equations for estimating the period of vibration of existing buildings. *Proceedings of the First European conference on earthquake engineering and seismology*. Vol. 1122. 2006.

